



# Detection and Classification of Brain Tumor in MRI Images Using Wavelet Transform and Convolutional Neural Network

**Ahmad M. Sarhan<sup>1\*</sup>**

<sup>1</sup>*Department of Computer Engineering, Amman Arab University, Amman, Jordan.*

## **Author's contribution**

*The sole author designed, analysed, interpreted and prepared the manuscript.*

## **Article Information**

DOI: 10.9734/JAMMR/2020/v32i1230539

### Editor(s):

(1) Syed Faisal Zaidi, King Saud Bin Abdulaziz University-HS, Saudi Arabia.

### Reviewers:

(1) K. P. Mredula, Sardar Vallabhbhai Patel Institute of Technology, India.

(2) S. Sahand Mohammadi Ziabari, TU Delft University, Netherlands.

(3) Akhilesh Pandey, Kanpur Institute of Technology, India.

Complete Peer review History: <http://www.sdiarticle4.com/review-history/58115>

**Original Research Article**

**Received 06 May 2020**

**Accepted 12 July 2020**

**Published 30 July 2020**

## **ABSTRACT**

A brain tumor is a mass of abnormal cells in the brain. Brain tumors can be benign or malignant. Conventional diagnosis of a brain tumor by the radiologist, is done by examining a set of images produced by magnetic resonance imaging (MRI). Many computer-aided detection (CAD) systems have been developed in order to help the radiologist reach his goal of correctly classifying the MRI image. Convolutional neural networks (CNNs) have been widely used in the classification of medical images. This paper presents a novel CAD technique for the classification of brain tumors in MRI images. The proposed system extracts features from the brain MRI images by utilizing the strong energy compactness property exhibited by the Discrete Wavelet transform (DWT). The Wavelet features are then applied to a CNN to classify the input MRI image. Experimental results indicate that the proposed approach outperforms other commonly used methods and gives an overall accuracy of 98.5%.

**Keywords:** *Brain tumor; cancer detection; wavelet transform; Convolutional Neural Networks (CNNs); Magnetic Resonance Imaging (MRI).*

\*Corresponding author: E-mail: [asarhan@hotmail.com](mailto:asarhan@hotmail.com);

## 1. INTRODUCTION

Brain tumor results from cancer cells that grow uncontrollably in the brain to create a mass of cancer tissue (tumor). The tumor in the brain interferes with brain tasks such as memory, muscle control, and other body operations [1-2]. Depending on the type of tumor and its location in the brain, symptoms may include seizures, memory problems, unusual behavior, confusion, vision changes, and balance difficulties [3-5]. Brain cancer may be caused by factors such as exposure to ionizing radiation and a family history of brain cancer [6-7]. Several studies claim that there is a link between cell phones and brain cancer.

Various treatment options are available for brain cancer patients. The options include radiation therapy, surgery, chemotherapy, or a combination of these treatments [8]. Usually the first stage of treatment given to brain cancer patients is radiotherapy [9-10].

The second stage of thereby is a surgery which aims to remove all of the tumor. However, if some tumor is left after surgery, which is often the case, then chemotherapy is administered [11-12].

Magnetic Resonance Imaging (MRI) is the preferred way to diagnose a brain tumor, as it generates more detailed pictures than computerized tomography (CT) scans [13]. MRI is a non-invasive and painless scanning technique. Depending on the type of tumor suspected, the physician may order MRI for the brain, spinal cord, or both [14].

According to the WHO (World Health Organization), brain tumors are classified into two general types: benign (noncancerous) and malignant (cancerous) [15-17]. Malignant tumors are subsequently classified into grade s(I through IV.) Grade-I tumor, the least aggressive type, is called Pilocytic Astrocytoma. Grade-II tumor is a low-grade Astrocytoma; Grade-III tumor is called Anaplastic Astrocytoma. Grade-IV tumor, the most aggressive type, is called Glioblastoma [18-19].

Presented in this paper is a novel brain cancer classification system based on Wavelet decomposition and Convolutional Neural Networks (CNNs). Specifically, this study, addresses the classification of three types of brain tumors (meningioma, glioma, and pituitary

tumor). T1-weighted contrast-enhanced MRI (CE-MRI) images are adopted in this paper.

Experimental results show that the proposed WCNN system outperforms commonly proposed systems such as the Support Vector machines (SVM). The proposed system produces a high accuracy rate of 98.5%.

### 1.1 The State of the Art in Brain Tumor Classification

The following detailed classification of brain tumors, according to the WHO, is associated with cell origin and behavior:

- Astrocytoma, which develop from star-shaped cells called astrocytes, are the most common central nervous system (CNS) tumors. Astrocytoma arise anywhere in the spinal cord or brain. In adults, astrocytomas often occur in the cerebrum, the largest part of the brain, that controls speech, movement, learning, thinking and reading.
- Brain stem gliomas, a high-grade astrocytomas, originate in the brain stem (the lowest part of the brain that connects the spinal cord. to the brain). Brain stem gliomas affect several functions such as breathing, blood pressure, hunger, and body temperature. Tumors in this area can be difficult to treat.
- Glioblastoma, a grade IV astrocytoma, is an aggressive type of CNS tumor that originates in the supportive tissue of the brain and usually affects adults. Glioblastoma, which is considered the most common grade IV brain cancer, may form in any lobe of the brain, but they often develop in the frontal and temporal lobes.
- Meningioma form in the membrane that surrounds the spinal cord and the brain. They are non-cancerous (benign) and are often removed with surgery. Some meningiomas may not need treatment at all.
- Ependymomas often develop in the spinal cord and the lining of the ventricles. They are most common in adolescents and children.
- Oligodendrogliomas, a rare type of slow-growing tumor. They originate in the cells that produce myelin (the fatty coating that keeps nerves in the brain and spinal cord). These tumors often occur in the cerebrum of middle-aged adults. As shown by Table 1, several MRI brain datasets have been used by researchers and are available online.

Conventional cancer detection techniques examine the tissue of the tumor to form a judgment as to the tumor type [20-21]. However, many tumors do not possess distinctive morphological characteristics that are essential for differential classification. Hence, the assessment of histopathological and clinical information may lead to a misdiagnosis. Thus, there is a strong demand for automatic methods to perform brain tumor detection and classification.

Computer aided detection (CAD) systems, especially those systems based on machine learning and artificial intelligence (AI) methods, have been widely adopted in cancer detection systems [22]. Some studies claim that AI systems have outperformed humans in many imaging areas in medicine [23-24]. CAD systems offer many advantages. In addition to providing a fast screening process, CAD systems improve the subjective interpretation of radiologists. As with other fields of medical imaging, CAD systems that are used in brain tumor detection and classification, are significantly based on machine learning and AI software. A variety of CAD techniques have been proposed in the literature for the diagnosis and classification of brain tumor. Segmentation is perhaps the most common preprocessing step among these techniques, and is used to extract the infected region of the brain from the input MRI image.

A review of brain tumor segmentation methods is given by Tiwari [25]. Hakeel et al. used a wireless infrared imaging sensor for brain tumor

detection [26]. Maalini et al. used morphological reconstruction and thresholding for Brain tumor extraction [27]. Jemimma et al. performed brain tumor segmentation using the Watershed algorithm based DAPP features [28]. Yin et al. employed a whale optimization algorithm for brain tumor classification [29]. Gurbină et al. [30] and Shree et al. [31] used Wavelet for brain tumor identification.

## 2. MATERIALS AND METHODS

Proposed in this paper is a Wavelet-based CNN (WCNN) system for brain tumor detection and classification. MRI images, which are the most popular imaging technique for brain tumor scanning, are used in this study. A block diagram showing the main stages of the proposed system is depicted in Fig. 1.

The cascade functions performed by the proposed system start by taking the Wavelet decomposition of the input image  $I$ , which is an MRI image and it represents any image in the employed brain tumor dataset.

Magnetic resonance imaging (MRI) is a medical imaging technique that uses a strong magnetic field and radio waves to create detailed images of the body organs and tissues.

MRI allows for the detailed visualization of the brain and spinal cord anatomy in all three planes: axial, sagittal and coronal. The most common MRI relaxation time scans are the T1-weighted (T1) and T2-weighted (T2) scans. If ordered, the

**Table 1. MRI brain databases**

#	Database	Location
1	BRAINIX medical images	<a href="https://www.medicalimages.com/search/brain.html">https://www.medicalimages.com/search/brain.html</a>
2	TCGA-GBM, TCGA-LGG	<a href="https://wiki.cancerimagingarchive.net/display/Public/TCGA-LGG">https://wiki.cancerimagingarchive.net/display/Public/TCGA-LGG</a>
3	Figshare (Cheng)	<a href="https://figshare.com/articles/brain_tumor_dataset/1512427">https://figshare.com/articles/brain_tumor_dataset/1512427</a>
4	Harvard Medical School	<a href="http://med.harvard.edu/AANLIB/">(http://med.harvard.edu/AANLIB/</a>
5	Moffitt Cancer Research Center	<a href="https://moffitt.org/">https://moffitt.org/</a>
6	BraTS 2013,2014,2016,2018,2020	<a href="https://ipp.cbica.upenn.edu/">https://ipp.cbica.upenn.edu/</a>

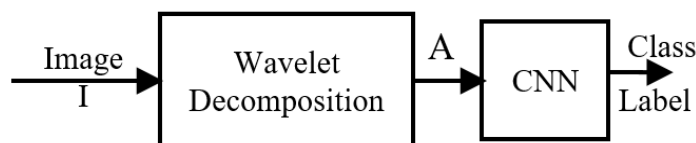


**Fig. 1. Block diagram of the proposed system**

MRI can also generate other scans such as T1-weighted contrast-enhanced (T1c), and T2-weighted Fluid Attenuated Inversion Recovery (FLAIR) images [32].

## 2.1 Image Dataset

The brain tumor database was obtained from figshare (Cheng) collection. This brain tumor database contains T1-weighted contrast-enhanced images from 233 patients with three types of brain diseases. Specifically, this dataset contains 1426 slices representing glioma, 930 slices representing pituitary tumor, and 708 slices representing meningioma. In this study, only 170 images from each class were used; 70% for training and 30% for testing. Table 2 summarizes the dataset details. Sample images from each class of the database are shown in Fig. 2.

Unlike most of the brain classification CAD methods which require segmenting the input image before classifying it, the proposed WCNN method operates on the whole input image without doing any segmentation to it. Therefore, the proposed system significantly reduces the time complexity of the classification system and avoids any potential errors which may occur in the segmentation phase. The first phase of the proposed system is to use the Wavelet transform to obtain discriminative features from the input image.

## 2.2 Wavelet Transform

The Wavelet Transform (Wavelet decomposition), is a lossless transform. The transform of an image gives another way of representing the image. It does not change the energy or information content of the image. [33] The Wavelet decomposition tree, shown in Fig. 3, illustrates the functions of the Wavelet decomposition transform. The input image, at the first level of decomposition, produces two vectors of coefficients: approximation and detail coefficients. The approximation coefficients represent the low frequency contents of the signal, while the detail coefficients represent the high-frequency components. In the second level of decomposition, the approximation coefficients produce two sets of approximation and detail coefficients, whose lengths are equal to half of the length of the original approximation vector. The process of decomposition further divides the approximation coefficients into two new vectors for each subsequent level of decomposition.

To show the decomposition operations employed by Wavelet transform, Fig. 4 depicts Wavelet decomposition details of a sample image using the Haar Wavelet. The decomposed image was obtained from the meningioma images and is shown in Fig. 2(a). The Haar Wavelet which is also known as the db1 Wavelet, is considered the first and simplest Wavelet. The db1 wave looks like a step function [34].

**Table 2. Dataset labels and diseases**

Disease type	Class label	Number of images	Matrix size
meningioma,	1	170	512 × 512
glioma	2	170	512 × 512
pituitary tumor	3	170	512 × 512

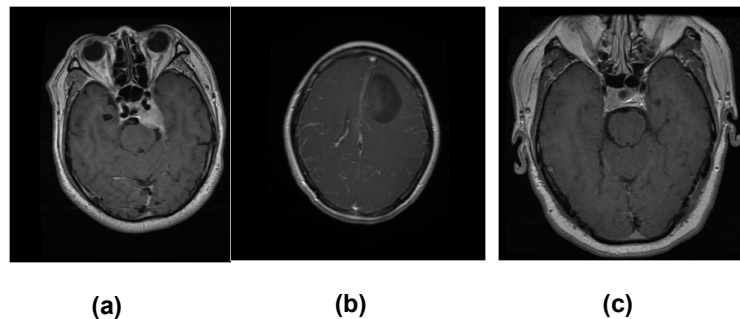


**Fig. 2. Sample images from the employed dataset: (a) Meningioma, (b) Glioma and (c) Pituitary tumor**

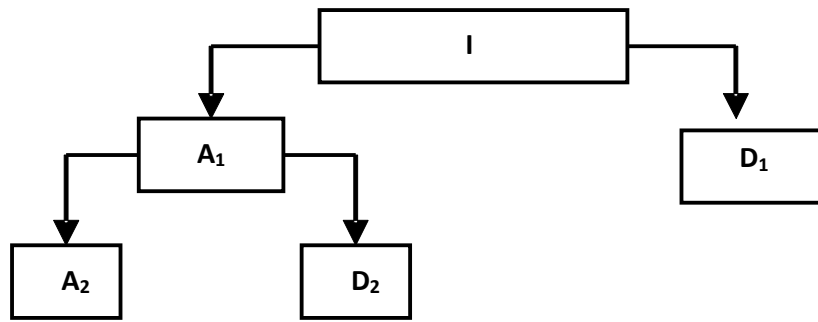


**Fig. 3. Wavelet decomposition tree. Variables  $I$ ,  $A_1$  and  $D_1$  represent the original image, approximation and detail coefficients at level 1, respectively**

The powerful capability of the Wavelet transforms to compress the image energy makes it suitable for image feature extraction applications [35].

Finally, the feature vector (approximation coefficients) is presented to a CNN and a SVM for classification. The same sets of inputs and outputs are used to train the SVM and the proposed WCNN system.

### 2.3 Conventional Neural Network

A Convolutional Neural Network (CNN) is a special type of Artificial Neural Network (ANN)

The original ANNs, such as the multilayer perceptron (MLP), have been very successful in pattern recognition applications [36-40]. ANNs have inspired the creation of CNN, a Deep learning algorithm.

Deep Learning is a branch of Machine Learning that employs Deep Neural Networks; neural networks with many layers. The CNN can be thought of as an ANN where at least one layer applies a convolution operation before it passes its output to the next layer [41]. Commonly, the mean value and the max value functions are used in the convolution operation, but other functions could also be used. CNNs present a

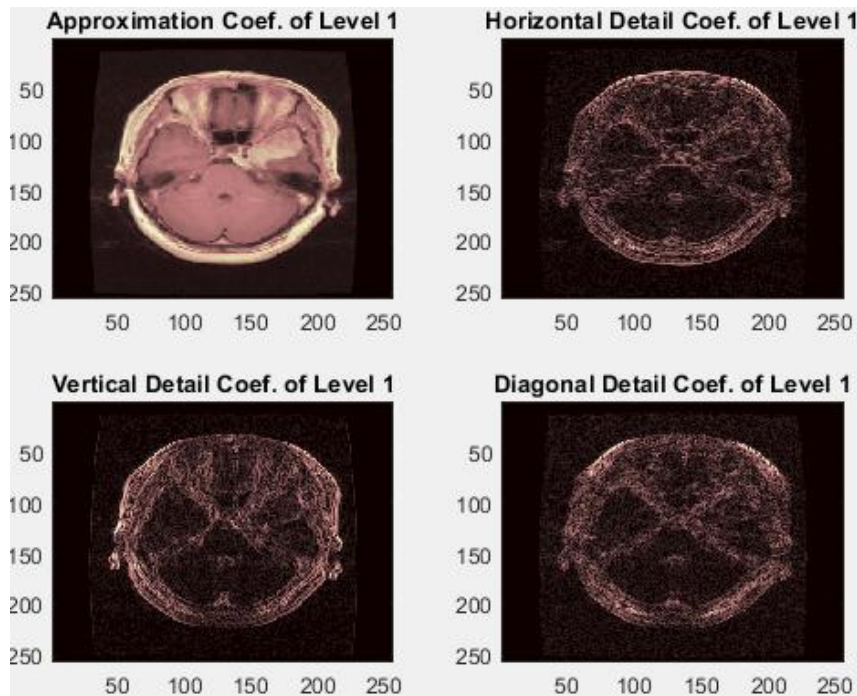


**Fig. 4. Wavelet decomposition of a meningioma image using the Haar Wavelet**

quantum leap in the area of image classification and computer vision. A very famous CNN design is the AlexNet [42] which has shown superior performance in general image recognition applications.

The basic structure of a CNN consists of three components: convolutional layer, pooling layer, and output layer. The convolutional layer scans the whole image, using a moving window approach, to create a feature map. The Pooling layer samples the output of the convolutional layer which reduces the amount of data to be learned. The use of the convolutional and pooling layers is often repeated several times. Fully connected input layer converts the outputs generated by previous layers into a single vector to be applied to the next layer. Fully connected layer produces a weighted sum of the input generated by the feature analysis to predict an output label. The Fully connect delayer determines the output class. A typical CNN architecture is depicted in Fig. 5.

As indicated by Fig. 5, the typical input to a CNN is an image of size  $m \times m \times r$ , where  $r$  is the number of channels ( $r=1$  for gray-scale and  $r=3$  for RGB images). Normally, the CNN has the capability to perform image classification using raw images as direct inputs. However, the implementation of the CNN in the proposed WCNN system uses Wavelet features as inputs to the CNN. This process greatly reduces the number of features; and therefore, makes the learning task of the CNN much easier.

The architecture of the proposed CNN classifier contains five layers: input layer, convolutional layer, max pooling layer, fully connected layer, and output layer.

Specifically, the input layer has a size of  $128 \times 8 \times 128$  corresponding to the size of the approximation matrices. The output layer had 3 neurons corresponding to the number of classes. Next, we compare the performance of the proposed WCNN system to that of a SVM system.

#### 2.4. Support Vector Machine Implementation

Like CNNs, SVMs are supervised learning algorithms that have been widely implemented in classification applications. SVMs were originally proposed by Cortes et al. [43-44]. A SVM was originally designed to be a binary or wo-class classifier.

However, SVMs have been altered to tackle data composed of more than two classes [45-46]. SVMs have shown remarkable success in solving linear and non-linear classification problems. As depicted in Fig. 6, a SVM classifies data by determining the best hyperplane that isolates the data points of the two classes. In other words, an SVM tries to find the widest possible margin that separates the two classes with no interior data points.

The SVM algorithm implemented here uses the Gaussian kernel defined by:

$$k(x, y) = \exp\left(-\frac{\|x - y\|^2}{2\sigma^2}\right),$$

where  $\sigma$  is a user-defined variance parameter.

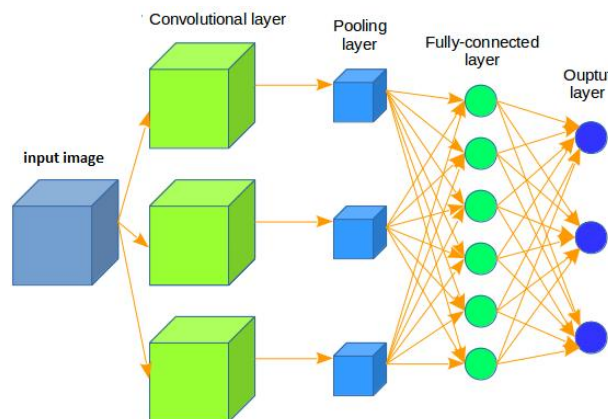


Fig. 5. Structure of a typical CNN

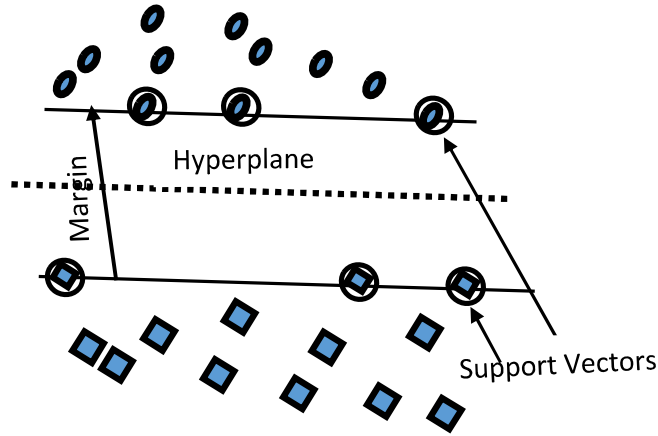


Fig. 6. Support vector machine

### 3. DISCUSSION AND RESULTS

About 70% of data were used for training and 30% for testing. The proposed system attempts to classify an input image into one of the three classes (meningioma, glioma, and pituitary tumor). The traces of loss and accuracy of the proposed system are shown in Fig. 7.

The maximum success rate (accuracy) of the proposed WCNN system for this experiment is 98.5%. In the next experiments, we investigate the effects of using different wavelets on the accuracy. Figs 8 and 9 show the success rates when using the Daubechies (dB) and the Symmetric (sym) wavelets, respectively.

To show the validity of the proposed system, its accuracy is compared to the SVM classifier. When operating on the same feature matrices as the proposed WCNN system, the SVM system produced an accuracy of 92.5%.

Several statistical measures are used to analyze the performance of the proposed WCNN system. Specifically, the performance of the proposed algorithm is evaluated by computing the percentages of sensitivity (SE), specificity (SP) and accuracy (ACC) as follows:

Sensitivity: is the fraction of real events that are correctly detected among all real events and is given by:

$$SE = \frac{TPX 100}{(TP + FN)}$$

Specificity is defined as the fraction of nonevents that are correctly rejected and is given by:

$$SP = \frac{TNX 100}{(TN + FP)}$$

Accuracy is the fraction of the real events that are correctly detected and the non-events that are correctly rejected, among all events and non-events and is defined as:

$$ACC = \frac{(TP + TN) X 100}{(TP + TN + FP + FN)}$$

where,

FP: number of false positive specimens (predicts non-tumor as tumor).

TP: number of true positive specimens (predicts tumor as tumor).

FN: number of false negative specimens (predicts tumor as non-tumor).

TN: number of true negative specimens (predicts non-tumor as non-tumor).

The prevalence is determined from the sensitivity, specificity, and accuracy.

The calculated SE, SP, AC, and prevalence are given in Table 3.

Table 3 shows that the proposed system produces high sensitivity and specificity values, indicating that the system is robust and reliable.

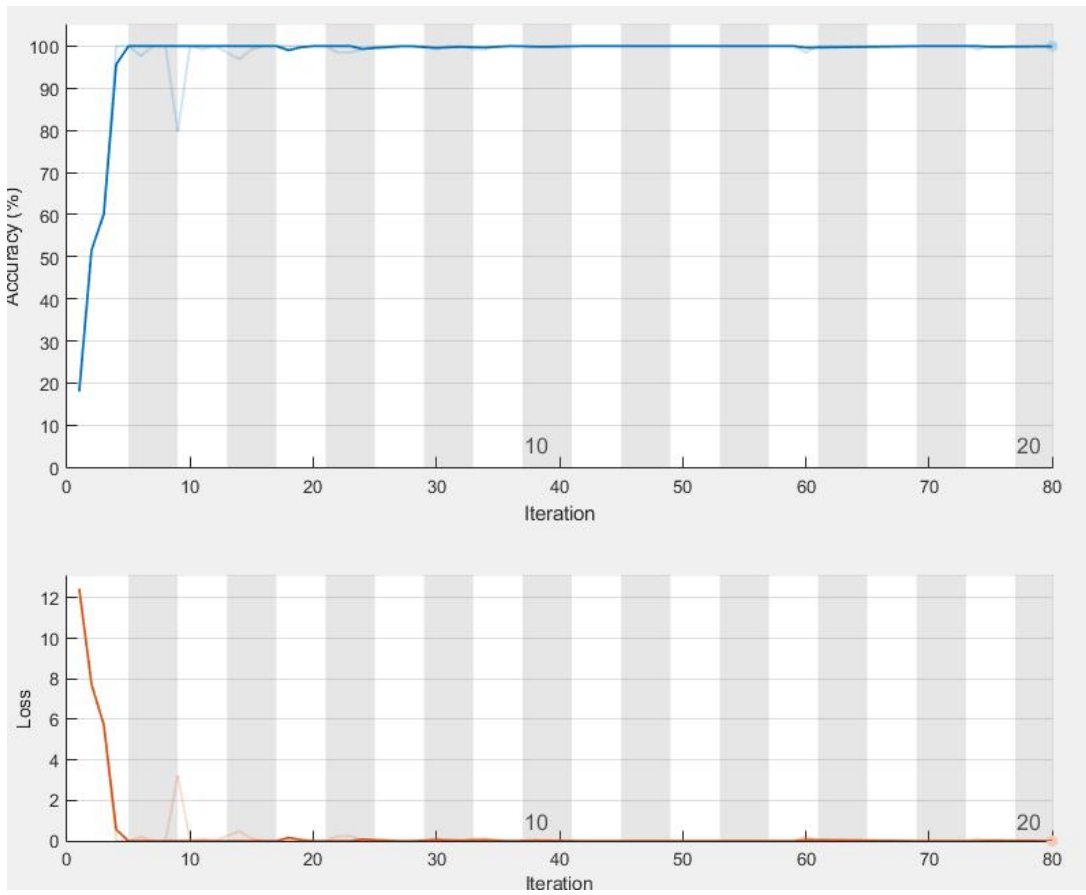


Fig. 7. Traces of accuracy and loss during training

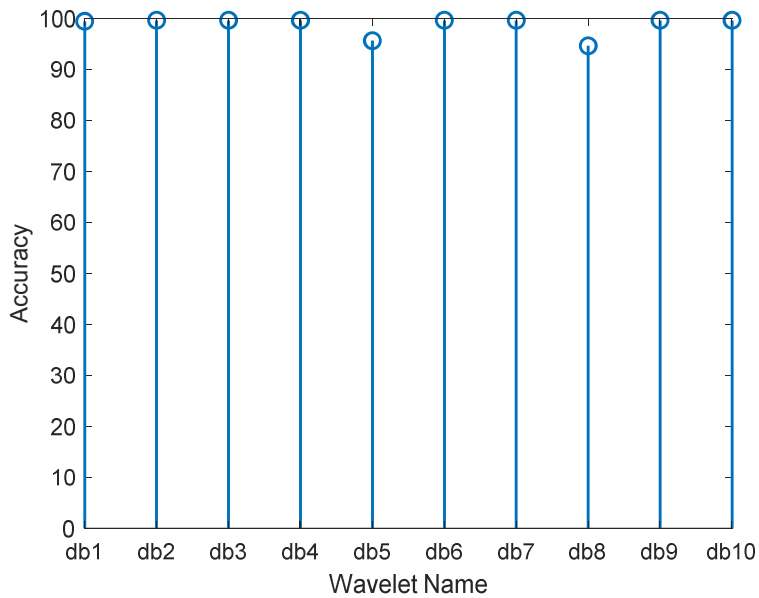
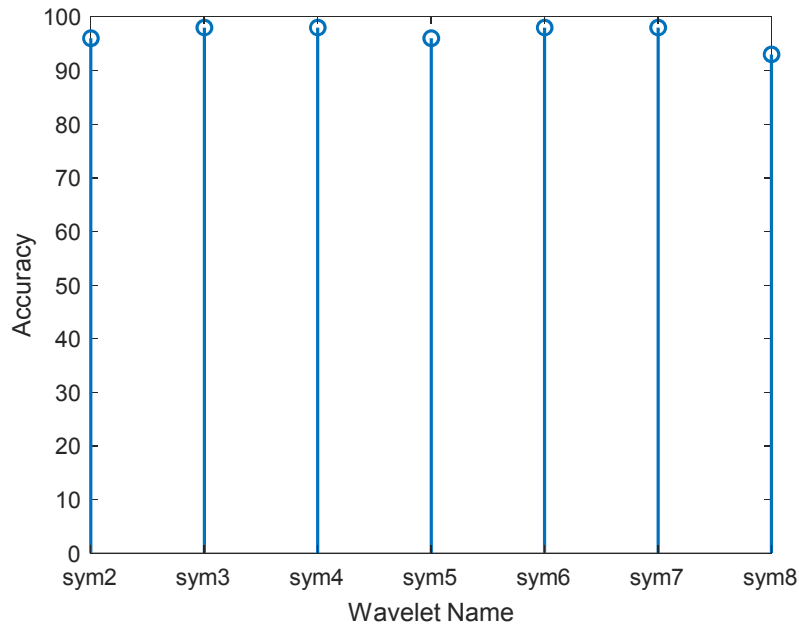


Fig. 8. Accuracy using daubechies wavelets



**Fig. 9. Accuracy using symmetric wavelets**

**Table 3. Performance metrics of the proposed system**

No. of cases	SE	SP	ACC	Prevalence
100	95.5%	92.5 %	98.5%	2

#### 4. CONCLUSION

In this paper, a novel approach to the classification of Brain cancer using Deep Neural Network is presented and developed. Most of the systems that are currently proposed in the literature, segment the input Brain image before applying it to the CNN classifier. The proposed CNN system processes the whole Brain image with Wavelet decomposition, without doing any segmentation to the input image. Hence, the proposed system has a lower time complexity than the other systems proposed in the literature. Wavelet decomposition highly reduces the dimensions of the input image, which in turn, simplifies the work of the CNN classifier. The proposed system classifies the input Brain image to one of three classes: meningioma, glioma, and pituitary tumor.

The Brain images are MRI scans taken from the Figshare(Cheng) database. To show the validity and robustness of the proposed system, its performance is compared to the SVM classifier. Both the proposed WCNN system and the SVM

classifier received the same feature vectors as input.

Experimental tests on the Figshare (Cheng) database achieved 98.5% of recognition accuracy using a decomposition level of two and the Haar wavelet. Simulation results have indicated that the proposed system always produces higher success rates than the SVM system.

#### CONSENT

As per international standard written participant consent has been collected and preserved by the authors.

#### ETHICAL APPROVAL

As per international standard written ethical permission has been collected and preserved by the author(s).

#### COMPETING INTERESTS

Author has declared that no competing interests exist.

## REFERENCES

1. The American Cancer Society. Available: <https://www.cancer.org/>
2. Komori, T. Updating the grading criteria for adult diffuse gliomas: beyond the WHO2016CNS classification. *Brain Tumor Pathol*; 2020.
3. Koriyama S, Nitta M, Kobayashi T, et al. A surgical strategy for lower grade gliomas using intraoperative molecular diagnosis. *Brain Tumor Pathol*. 2018;35: 159–167.
4. Ogawa K, Kurose A, Kamataki A, et al. Giant cell glioblastoma is a distinctive subtype of glioma characterized by vulnerability to DNA damage. *Brain Tumor Pathol*. 2020;37:5–13.
5. Asano K, Kurose A, Kamataki A, et al. Importance and accuracy of intraoperative frozen section diagnosis of the resection margin for effective carmustine wafer implantation. *Brain Tumor Pathol*. 2018;35: 131–140.
6. Yokogami K, Yamasaki K, Matsumoto F, et al. Impact of PCR-based molecular analysis in daily diagnosis for the patient with gliomas. *Brain Tumor Pathol*. 2018;35:141–147.
7. Góes P, Santos BFO, Suzuki FS et al. Necrosis is a consistent factor to recurrence of meningiomas: should it be a stand-alone grading criterion for grade II meningioma? *J Neurooncol*; 2017.
8. Sasaki S, Tomomasa R, Nobusawa S, et al. Anaplastic pleomorphic xanthoastrocytoma associated with an H3G34 mutation: a case report with review of literature. *Brain Tumor Pathol*. 2019;36:169–173.
9. Tan CL, Vellayappan B, Wu B, et al. Molecular profiling of different glioma specimens from an Ollier disease patient suggests a multifocal disease process in the setting of IDH mosaicism. *Brain Tumor Pathol*. 2018;35:202–208.
10. Yamasaki T, Sakai N, Shinmura K, et al. Anaplastic changes of diffuse leptomeningeal glioneuronal tumor with polar spongioblastoma pattern. *Brain Tumor Pathol*. 2018;35:209–216.
11. Girolami I, Cima L, Ghimenton C, et al. NRAS mutated diffuse leptomeningeal melanomatosis in an adult patient with a brief review of the so-called “forme fruste” of neurocutaneous melanosis. *Brain Tumor Pathol*. 2018;35:217–223.
12. Louis DN. A feast of reviews about brain and pituitary tumor pathology. *Brain Tumor Pathol*. 2018;35:49–50. Available: <https://doi.org/10.1007/s10014-018-0315-2>.
13. Saeed Jerban, Eric Y. Chang, Jiang Du, “Magnetic resonance imaging (MRI) studies of knee joint under mechanical loading: Review,” *Magnetic Resonance Imaging*. 2020;65:27-36.
14. Anjali Wadhwa, Anuj Bhardwaj, Vivek Singh Verma, A review on brain tumor segmentation of MRI images, *Magnetic Resonance Imaging*. 2019;61:247-259.
15. Nishioka H, Inoshita N. New WHO classification of pituitary adenomas (4th edition): Assessment of pituitary transcription factors and the prognostic histological factors. *Brain Tumor Pathol*. 2018;35:57–61.
16. Iuchi T, Sugiyama T, Ohira M, et al. Clinical significance of the 2016 WHO classification in Japanese patients with gliomas. *Brain Tumor Pathol*. 2018;35:71–80.
17. Shibuya, M. Welcoming the new WHO classification of pituitary tumors 2017: revolution in TTF-1-positive posterior pituitary tumors. *Brain Tumor Pathol*. 2018;35:62–70.
18. Akagi Y, Yoshimoto K, Hata N, et al. Reclassification of 400 consecutive glioma cases based on the revised 2016WHO classification. *Brain Tumor Pathol*. 2018;35:81–89.
19. Kuwahara K, Ohba S, Nakae S, et al. Clinical, histopathological, and molecular analyses of IDH-wild-type WHO grade II–III gliomas to establish genetic predictors of poor prognosis. *Brain Tumor Pathol*. 2019;36, 135–143 (2019).
20. Barresi V, Lioni S, Caliri S, et al. Histopathological features to define atypical meningioma: What does really matter for prognosis?. *Brain Tumor Pathol*. 2018;35: 168–180.
21. Nambirajan A, Malgulwar PB, Sharma A, et al. Clinicopathological evaluation of PD-L1 expression and cytotoxic T-lymphocyte infiltrates across intracranial molecular subgroups of ependymomas: Are these tumors potential candidates for immune check-point blockade?. *Brain Tumor Pathol*. 2019;36:152–161.
22. Challen R, Denny J, Pitt M, Gompels L, Edwards T, Tsaneva-Atanasova K.

- Artificial intelligence, bias and clinical safety. *BMJ Qual Saf.* 2019;28:231–37.3.
23. Crawford K, Calo R. There is a blind spot in AI research. *Nature.* 2016;538:311–13.4.
  24. Lallas A, Argenziano G. Artificial intelligence and melanoma diagnosis: ignoring human nature may lead to false predictions. *Dermatol Pract Concept.* 2018; 8:249–51.5
  25. Tiwari A, Srivastava S, Pant M. Brain tumor segmentation and classification from magnetic resonance images: Review of selected methods from 2014 to 2019. *Pattern Recognition Letters*; 2019. Available:<https://doi.org/10.1016/j.patrec.2019.11.020>
  26. hakeel PM, Tobely TEEL, Al-feel H, Manogaran G, Baskar S. Neural network based brain tumor detection using wireless infrared imagingsensor. In *IEEE Access.* 2019;7:5577–5588. Available:<https://ieeexplore.ieee.org/document/8599180>
  27. Maalinii GB, Jatti A. Brain tumour extraction using morphological reconstruction and thresholding," *Materials Today Proceedings.* 2018;5(4):10689–10696. Available:<https://doi.org/10.1016/j.matpr.2017.12.350>.
  28. Jemimma TA, Vetharaj YJ. Watershed algorithm based DAPP features for brain tumor segmentation and classification. In *2018 International Conference on Smart Systems and Inventive Technology.* 2018;155158. Available:<https://ieeexplore.ieee.org/document/8748436>.
  29. Yin B, Wang C, Abza F. New brain tumor classification method based on an improved version of whale optimization algorithm. *Biomedical Signal Processing and Control.* 2019;56:101728. Available:<https://doi.org/10.1016/j.bspc.2019.10.010>
  30. Gurbină M, Lascu M, Lascu D. Tumor detection and classification of MRI brain image using different wavelet transforms and support vector machines. 2019;505–508. <https://ieeexplore.ieee.org/abstract/document/8769040>.
  31. Shree NV. Identification and classification of brain tumor MRI images with feature extraction using DWT and probabilistic neural network. *Brian Informatics.* 2018;5(1):23–30. Available:<https://doi.org/10.1007/s40708-017-0075-5.pdf>
  32. Stachera M, Sznajder K. *Magnetic resonance in human brain examinations: A brief outline of the techniques.* Utrecht: Cornell University; 2014.
  33. Ahmad M. Sarhan, Radaan Al-Dosari, Mammogram classification using discrete wavelet transform features and a novel vector quantization technique for breast cancer detection, *British Journal of Applied Science & Technology.* 2017;19(1).
  34. Ahmad M. Sarhan. A WPD scanning technique for iris recognition, *International Journal of Computer Applications.* 2014;85(14):6-12.
  35. Ahmad M. Sarhan. Wavelet-based feature extraction for DNA microarray classification, *Artificial Intelligence Review (Springer).* 2013;39(3):237-249.
  36. Khalid A. Buragga, Sultan Aljahdali, Sarhan AM. An Efficient Technique for Iris Recognition using Wavelets and Artificial Neural Networks," In *Proceedings of CATA 2015, Hawaii, USA; 2015.*
  37. Ahmad M. Sarhan. A comparison of vector quantization and artificial neural network techniques in typed Arabic character recognition," *International Journal of Applied Engineering Research (IJAER).* 2009;4(5):805-817.
  38. Sarhan AM. Optimal statistical artificial neural networks for Arabic character recognition," In *Proceedings of 16th Int'l Conference on Computers and Their Applications, Cancun, Mexico. 2008;53-58.*
  39. Sarhan AM, Al-Helalat OI. Probabilistic artificial neural networks for Arabic character recognition, In *Proceedings of 16th Int'l Conference on Software Engineering and Data Engineering, Las Vegas; 2007.*
  40. Sarhan AM, Al-Helalat OI. Arabic character recognition using artificial neural networks and statistical analysis," In *Proceedings of the ICCESSE Conference.* 2007;32-36.
  41. Huang G, Liu Z, Pleiss G, Van Der Maaten L, Weinberger K. Convolutional Networks with Dense Connectivity, *IEEE Trans. Pattern Anal. and Mach. Intell;* 2019.
  42. Han X, Zhong Y, Cao L, Zhang L. Pre-trained AlexNet architecture with pyramid pooling and supervision for high spatial resolution remote sensing image scene classification. *Remote Sens.* 2017;9: 848.

- Available:<https://doi.org/10.3390/rs9080848>
43. Cortes C, Vapnik V. Support vector networks," Machine Learning. 1995;20: 273-297,  
Liu X, Faes L, Kale A, et al. A comparison of deep learning performance against health care professionals in detecting diseases from medical imaging: a systematic review and meta-analysis. Lancet Digital Health; 2019.  
Available:[https://doi.org/10.1016/S2589-7500\(19\)30123-2.2](https://doi.org/10.1016/S2589-7500(19)30123-2.2)
44. Segera, Davies, Mbuthia, Mwangi, Nyete, Abraham. TI - Particle Swarm Optimized Hybrid Kernel-Based Multiclass Support Vector Machine for Microarray Cancer Data Analysis," BioMed Research International. 2019.
45. Ahmad M. Sarhan. A novel gene-based cancer diagnosis with wavelets and support vector machines, European Journal of Scientific Research (EJSR). 2010;46(4): 488-502.
46. Wang L. (Ed.). Support vector machines: Theory and applications vector machines. Computer Science. 2005;177: 6221.  
Available:<https://www.springer.com/gp/book/9783540243885>

© 2020 Sarhan; This is an Open Access article distributed under the terms of the Creative Commons Attribution License (<http://creativecommons.org/licenses/by/4.0>), which permits unrestricted use, distribution, and reproduction in any medium, provided the original work is properly cited.

*Peer-review history:*  
*The peer review history for this paper can be accessed here:*  
<http://www.sdiarticle4.com/review-history/58115>